Inorganica Chimica Acta 372 (2011) 353–361

Contents lists available at ScienceDirect

Inorganica Chimica Acta

journal homepage: www.elsevier.com/locate/ica

Metallo-β-lactamase and phosphotriesterase activities of some zinc(II) complexes

Muthaiah Umayal, Govindasamy Mugesh *

Department of Inorganic and Physical Chemistry, Indian Institute of Science, Bangalore 560012, India

ARTICLE INFO

Article history:
Available online 5 April 2011

Dedicated to Prof. S.S. Krishnamurthy

Keywords:
Antibiotic resistance
Asymmetric ligands
Metallo-β-lactamase
Phosphotriesterase
Synthesis
Zinc(II) complexes

ABSTRACT

Metallo-β-lactamases (mβl) and phosphotriesterase (PTE) are zinc(II) enzymes, which hydrolyze the β-lactam antibiotics and toxic organophosphotriesters, respectively. In the present work, we have synthesized a few asymmetric phenolate-based ligands by sequential Mannich reaction and their corresponding zinc(II) complexes. These zinc(II) complexes were studied for their mβl and PTE activities. It is shown that the zinc(II) complexes can hydrolyze oxacillin, the β-lactam antibiotic, at much higher rates as compared to the hydrolysis of *p*-nitrophenyl diphenylphosphate (PNPDPP), the phosphotriester. Among the complexes studied, the binuclear asymmetric complex **1** having a water molecule coordinated to one of the zinc(II) ions exhibits much better mβl activity than the mononuclear complexes. However, the mononuclear zinc(II) complexes having labile chloride ions exhibit significant PTE activity, which can be ascribed to the replacement of chloride ions by hydroxide ions during hydrolysis reactions.

1. Introduction

Zinc, the second most abundant transition metal in biology, plays important roles in a variety of biological processes [1]. It is an essential trace element, which is required for growth, development and differentiation of all types of life [2]. It plays an important role in transcription of DNA, translation of RNA, etc. The strong Lewis acidity, rapid ligand exchange, flexible coordination geometry, lack of redox property and 'borderline' hard–soft behavior make zinc as a suitable element for biological systems [3]. Zinc plays catalytic, cocatalytic, structural and protein interface roles in proteins. The largest group of zinc enzymes is zinc hydrolases, which are capable of hydrolyzing a broad spectrum of substrates in different metabolic pathways [4]. The mononuclear zinc(II) enzymes such as carbonic anhydrase and carboxypeptidase A are well studied. The study of multinuclear zinc(II) enzymes are of current interest [5]. The zinc(II) bound water or hydroxide ion is essential for the hydrolytic activity. In this regard, studies on zinc(II) enzymes such as metallo-β-lactamases (mβl) and phosphotriesterase (PTE) attracted considerable attention as the binuclear active sites of these enzymes are comparable and also possess metal-bound water molecule (Fig. 1).

β-Lactam antibiotics are the most widely used class of antibiotics, and the bacterial enzymes that hydrolyze these antibiotics are known as β-lactamases (Scheme 1). β-lactamases are classified into serine-β-lactamases (sβl) and metallo-β-lactamases (mβl). The serine-β-lactamases possess an active site serine residue which is essential for its hydrolytic activity. Currently, the inhibitors namely clavulanic acid, sulbactam and tazobactam are known for sβl. However, bacteria have evolved the zinc(II) containing metallo-β-lactamases that are capable of hydrolyzing a variety of β-lactam antibiotics including the latest generation of cephalosporins and carbapenems (e.g. imipenem) [6,7]. These mβls exists as both mono- and binuclear zinc(II) enzymes (Fig. 1). To date, there are no clinically useful inhibitors for these enzymes. Therefore, understanding the mode of action of mβl and design of inhibitors are important.

Synthetic organophosphates have been widely used as plasticizers, petroleum additives, pesticides (e.g. paraoxon and parathion) and chemical warfare agents (e.g. sarin) [8–10]. These organophosphates are extremely toxic to mammals as they are known to inhibit acetylcholine esterase (AChE) [11]. This leads to the accumulation of the neurotransmitter, acetylcholine which results in nerve failure, paralysis and ultimately death. The enzyme phosphotriesterase (PTE) is known to hydrolyze these toxic organophosphorus triesters to less toxic diesters (Scheme. 1) [12,13]. PTE has been isolated from soil bacteria and is a binuclear zinc(II) enzyme (Fig. 1) [14]. To date, the natural substrate for PTE is not known. As PTE degrades toxic organophosphorous triesters, the design of synthetic analougues for PTE may lead to the development of catalysts for the degradation of such compounds. The active site of PTE consists of a binuclear zinc(II) site with metal-bound water molecule (Fig. 1). The ligand system employed in most of the synthetic analogs known for these enzymes mβl and PTE are symmetrical in nature [15–17]. As the metal ions are in different coordination environment in natural systems, we have synthesized some asymmetrical ligands and their corresponding zinc(II)

* Corresponding author.
E-mail address: mugesh@ipc.iisc.ernet.in (G. Mugesh).

0020-1693/$ - see front matter © 2011 Elsevier B.V. All rights reserved.
doi:10.1016/j.ica.2011.03.064

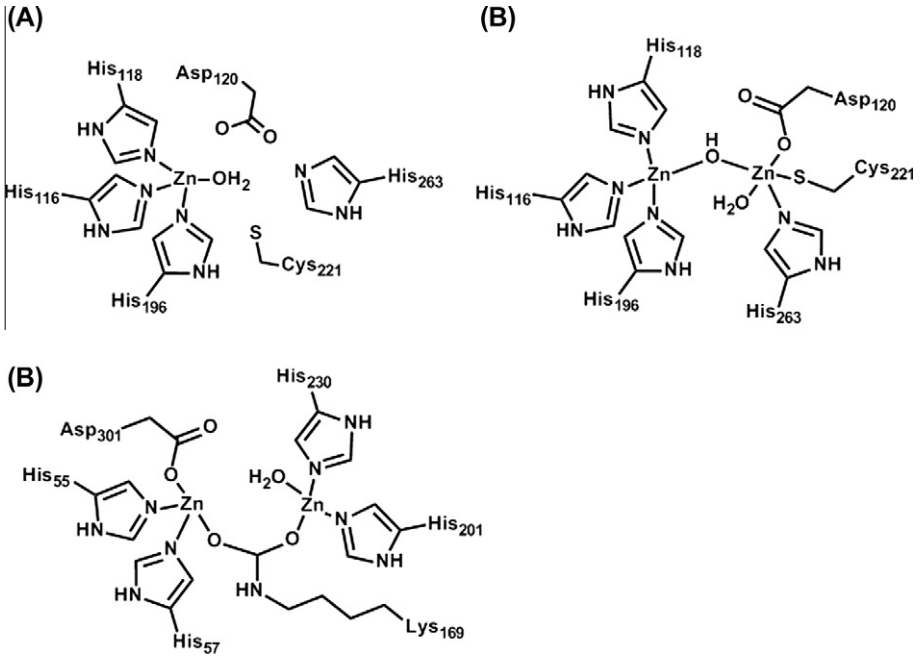

Fig. 1. Active sites of metallo-β-lactamase and phosphotriesterase. (A) and (B) represents mono- and binuclear active sites of metallo-β-lactamase, respectively, from *B. cereus*. (C) Represents the binuclear active site of phosphotriesterase from *Pseudomonas diminuta*. PDB codes for structures (A), (B) and (C) are 1BMC, 1BC2 and 1HZY, respectively [18–20].

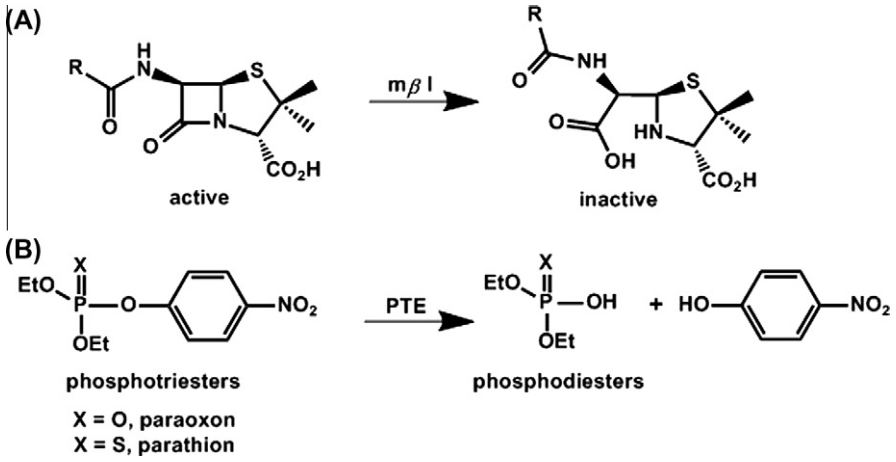

Scheme 1. Function of metallo-β-lactamase and phosphotriesterase. (A) Hydrolysis of β-lactam ring in antibiotics by metallo-β-lactamase. (B) Hydrolysis of organophosphotriesters to diesters by phosphotriesterase.

complexes. The mβl and PTE activities of the synthesized zinc(II) complexes were determined and compared with that of a known synthetic mimic.

2. Experimental

2.1. General procedure

Oxacillin (sodium salt) was obtained from Fluka; penicillanase (β-lactamae II, BCII) from *Bacillus cereus* was obtained from Sigma. Sodium hydride, HEPES sodium salt and CHES were obtained from Sigma–Aldrich Chemical Company. HPLC grade solvents for the kinetic experiments were obtained from Merck. *N,N*-dimethylamine, *N,N*-diethylamine and *N,N*-diproylamine, *p*-Cresol, paraformaldehyde and 37% formaldehyde solution were of highest purity purchased from local suppliers. Solvents were purified by standard procedures and were freshly distilled prior to use. The chemical reactions were carried out under nitrogen by using standard vacuum-line techniques. ^{1}H (400 MHz) and ^{13}C (100 MHz) NMR spectra were obtained by using a Bruker 400 NMR spectrometer. Chemical shifts are cited in ppm with respect to $SiMe_4$ as internal (^{1}H and ^{13}C) standard. Mass spectral studies were carried out by using either a Q-TOF micro mass spectrometer with ESI-MS mode analysis or a Bruker ESI-MS ion-trap. In the case of isotopic patterns, the value is given for the most intense peak. The synthesis of HL3, HL4, complex **4** and *p*-nitrophenyl diphenylphosphate (PNPDPP) were carried out by using reported procedures [15,17,21].

Thin-layer chromatography analyses were carried out on precoated silica gel plates (Merck) and spots were visualized by UV irradiation. Column chromatography was performed on glass

columns loaded with silica gel or an automated flash chromatography system (Biotage) by using preloaded silica cartridges. High performance liquid chromatography (HPLC) experiments were carried out on a Waters Alliance System (Milford, MA) consisting of a 2690 photodiode-array detector and a fraction collector. The assays were performed in 1.8 ml sample vials and a built-in autosampler was used for sample injection. The alliance HPLC system was controlled with EMPOWER software (Waters corporation, Milford, MA).

2.2. Synthesis of 2-((diethylamino)methyl)-4-methyl phenol

To a solution of *p*-cresol (2.9 mL, 27.8 mmol) and *N,N*-diethylamine (2.9 mL, 27.8 mmol) in 5 mL of ethanol, paraformaldehyde (835 mg, 27.8 mmol) was added. The reaction mixture was stirred at 80 °C for 3 h and it was monitored time to time by TLC for completion. The solvent was evaporated and the resulting oil was subjected to column chromatography by using petroleum ether and ethyl acetate as eluents. Yield: 2.8 g (52%). ^{1}H NMR ($CDCl_3$, ppm), δ 1.11 (t, 6H, J = 8 Hz), 2.25 (s, 3H), 2.62 (q, 4H, *J* = 4 Hz), 3.72 (s, 2H), 6.71 (d, 1H, *J* = 8 Hz), 6.78 (s, 1H), 6.96 (d, 1H, *J* = 8 Hz); ^{13}C NMR ($CDCl_3$, ppm), δ 11.7, 21.0, 46.7, 57.4, 116.2, 122.3, 128.3, 129.3, 129.4, 156.4.

2.3. Synthesis of 2-((diethylamino)methyl)-6-((dimethylamino) methyl)-4-methyl phenol (HL1)

To a solution of 2-((diethylamino)methyl)-4-methyl phenol (1000 mg, 5.2 mmol) and 40% aqueous *N,N*-dimethylamine (0.6 mL, 5.2 mmol), 37% formaldehyde aqueous solution (0.4 mL, 5.2 mmol) was added dropwise and the temperature was maintained below 30 °C (overall time was 30 min). After the mixture was stirred at room temperature for 1 h, it was stirred again between 45–55 °C for another 24 h. As the Mannich reaction is reversible, the formation of *p*-cresol was observed during the reaction. This led to the formation of the symmetrical ligands 2,6-((diethylamino)methyl)-4-methyl phenol and 2,6-((dimethylamino)methyl)-4-methyl phenol. To minimize the reversibility, the reaction was carried out at lower temperature and allowed to proceed for 48 h. To the resulting mixture, sodium chloride was added and stirring was continued for 20 min. The resulting oil was subjected to column chromatography by using petroleum ether and ethyl acetate. Yield: 0.18 g (14%). ^{1}H NMR ($CDCl_3$), δ 1.09 (t, 6H, *J* = 8 Hz), 2.22 (s, 3H), 2.34 (s, 6H), 2.62 (q, 4H, *J* = 8 Hz), 3.58 (s, 2H), 3.72 (s, 2H); ^{13}C NMR ($CDCl_3$, ppm) δ 11.5, 21.0, 44.9, 46.7, 55.9, 58.4, 122.4, 122.8, 128.0, 129.7, 130.9, 155.1; ESI-MS *Anal.* Calc. for $C_{15}H_{26}N_2O$ $[M+H]^+$: 251.2118. Found: 251.0314.

2.4. Synthesis of 2-((dipropylamino)methyl)-4-methyl phenol

To a solution of *p*-Cresol (2.9 mL, 27.8 mmol) and *N,N*-dipropylamine (3.8 mL, 27.8 mmol) in 5 mL of ethanol, paraformaldehyde (835 mg, 27.8 mmol) was added. The reaction mixture was stirred at 80 °C for 5 h and it was monitored by TLC till completion. The solvent was evaporated and the resulting oil was subjected to column chromatography by using petroleum ether and ethyl acetate as eluents. Yield: 3.67 g (60%). ^{1}H NMR ($CDCl_3$, ppm), δ 0.9 (t, 6H, *J* = 8 Hz), 1.52–1.59 (m, 4H), 2.24 (s, 3H), 2.45–2.49 (m, 4H), 3.71 (s, 2H), 6.71 (d, 1H, *J* = 8 Hz), 6.77 (s, 1H), 6.96 (d, 1H, *J* = 8 Hz); ^{13}C NMR ($CDCl_3$, ppm) δ 12.3, 20.0, 21.0, 55.9, 58.8, 116.2, 122.5, 128.4, 129.3, 129.4, 156.2.

2.5. Synthesis of 2-((dimethylamino)methyl)-6-((dipropylamino)-methyl)-4-methyl phenol (HL2)

To a solution of 2-((dipropylamino)methyl)-4-methyl phenol (1000 mg, 4.52 mmol) and 40% aqueous solution of *N,N*-dimethylamine (0.57 mL, 4.52 mmol), 37% formaldehyde aqueous solution (0.34 mL, 4.52 mmol) was added dropwise and the temperature was maintained below 30 °C (overall time was 30 min). After the mixture was stirred at room temperature for 1 h, the stirring was continued at temperatures between 45–55 °C for another 24 h. As the Mannich reaction was reversible under reaction conditions, the formation of *p*-cresol was observed. This led to the formation of the symmetrical ligands 2,6-((dipropylamino)methyl)-4-methyl phenol and 2,6-((dimethylamino)methyl)-4-methyl phenol. To minimize the reversibility, the reaction was carried out at lower temperature. Sodium chloride was added and stirring was continued for additional 20 min. The resulting oil was subjected to column chromatography by using petroleum ether and ethyl acetate as eluents. Yield: 0.2 g (16%). ^{1}H NMR ($CDCl_3$), δ 0.89 (t, 3H, *J* = 8 Hz), 1.57–1.66 (m, 4H), 2.24 (s, 3H), 2.53–2.57 (m, 10H), 3.81 (s, 2H), 3.89 (s, 2H), 6.93 (s, 2H), 7.07 (s, 2H); ^{13}C NMR ($CDCl_3$), δ 12.3, 19.8, 20.9, 45.3, 55.7, 57.3, 58.6, 122.8, 123.6, 127.7, 129.1, 130.4, 154.6; ESI-MS *Anal.* Calc. for $C_{17}H_{30}N_2O$ $[M+H]^+$: 279.2431. Found: 279.2436.

2.6. Synthesis of complex **1**

Complex **1** was synthesized from HL1 by following the reported procedure. The ligand HL1 (150 mg, 0.6 mmol) in dichloromethane (5 ml) together with 60% NaH (21.6 mg, 0.54 mmol) in hexane (15 ml) were mixed and stirred at room temperature for 1 h in nitrogen atmosphere to obtain the corresponding sodium phenolate (NaL1). $Zn(OAc)_2{\cdot}2H_2O$ (197.6 mg, 0.9 mmol) was then added and the stirring was continued for an additional 1 h. It resulted in a turbid solution from which complex **1** [$Zn_2L1(\mu\text{-}OAc)(OAc)_2(H_2O)$], was filtered off as a white solid. The product was dried under vacuum to obtain a white crystalline solid. It was dissolved in dichloromethane and kept for crystallization. On standing at room temperature, colorless needle shaped crystals suitable for X-ray analysis was obtained. Yield: 0.22 g (64%) ^{1}H NMR ($CDCl_3$), 1.35 (br s, 6H), 2.01 (br s, 9H), 2.19 (s, 3H), 2.38 (s, 6H), 3.09–3.17 (m, 4H), 3.68 (s, 2H), 4.05 (s, 2H), 6.79 (s, 1H), 6.81 (s, 1H); ^{13}C NMR ($CDCl_3$), 8.91, 20.73, 23.24, 30.19, 46.71, 47.31, 55.68, 63.85, 118.35, 123.54, 124.11, 130.74, 133.7, 162.84, 180.0; ESI-MS *Anal.* Calc. for $[Zn2L1+4H]^+$: 381.0863. Found: 381.1214.

2.7. Synthesis of complex **2**

Complex **2** was synthesized from HL2 by following the reported procedure [15]. The ligand HL2 (50 mg, 0.18 mmol) in dichloromethane (5 ml) together with 60% NaH (6.5 mg, 0.16 mmol) in hexane (10 ml) were mixed and stirred at room temperature for 1 h in nitrogen atmosphere to obtain the corresponding sodium phenolate (NaL1). Anhydrous $ZnCl_2$ (12.2 mg, 0.09 mmol) was then added and the stirring was continued for an additional 1 h. It resulted in a turbid solution from which complex **2** was filtered off as a white solid. The product was dried under vacuum to obtain a white crystalline solid. It was dissolved in dichloromethane and kept for crystallization. On standing at room temperature, colorless needle shaped crystals suitable for X-ray analysis was obtained. Yield: 0.045 g (60%).^{1}H NMR ($CDCl_3$), δ 0.98–1.02 (t, 6H), 1.76–1.87 (m, 4H), 2.18 (s, 3H), 2.46 (s, 3H), 2.96–3.01 (m, 4H), 3.63 (s, 2H), 4.14 (s, 2H), 6.79 (s, 1H), 6.82 (s, 1H); ^{13}C NMR ($CDCl_3$), δ 11.7, 17.7, 20.7, 47.7, 54.8, 58.2, 63.7, 117.8, 123.5, 125.0, 130.8, 133.8, 161.6; ESI-MS *Anal.* Calc. for $[ZnClL2+4H]^+$: 381.1629. Found: 381.0720.

2.8. Synthesis of complex **3**

Complex **3** was synthesized from HL3 by following the reported procedure [15]. The ligand HL2 (50 mg, 0.18 mmol) in dichloromethane (5 ml) together with 60% NaH (6.5 mg, 0.16 mmol) in hexane (10 ml) were mixed and stirred at room temperature for 1 h in nitrogen atmosphere to obtain the corresponding sodium phenolate (NaL1). Anhydrous $ZnCl_2$ (12.2 mg, 0.09 mmol) was then added and the stirring was continued for an additional 1 h. It resulted in a turbid solution from which complex **3** was filtered off as a white solid. The product was dried under vacuum to obtain a white crystalline solid. It was dissolved in dichloromethane and kept for crystallization. On standing at room temperature, colorless needle shaped crystals suitable for X-ray analysis was obtained. Yield: 0.06 g (80%). The crystal structure of complex **3** reveals the formation of an identical complex prepared by different procedure [21].

2.9. Single crystal X-ray crystallography

X-ray crystallographic studies were carried out on a Bruker CCD diffractometer with graphite-monochromatized Mo Kα radiation (λ = 0.71073 Å) controlled by a Pentium-based PC running on the SMART software package (Bruker AXS: Madison, WI) [22]. Single crystals were mounted at room temperature on the ends of glass fibers and data were collected at room temperature. The structures were solved by direct methods and refined using the SHELXTL software package (Siemens Industrial Automation Inc., Madison, WI) [23]. In general, all non-hydrogen atoms were refined anisotropically. Hydrogen atoms were assigned idealized locations. Empirical absorption corrections were applied to all structures using SADABS (Siemens Industrial Automation Inc., Madison, WI) [24].

2.10. Metallo-β-lactamase assay

The hydrolysis of oxacillin, the β-lactam substrate, by the zinc(II) complexes were determined by HPLC method [15]. The decrease in the concentration of the oxacillin was followed by measuring the peak area of oxacillin at 254 nm and the amount of oxacillin present in the solution at a given time is determined from the calibration plot obtained by injecting known concentrations of oxacillin. The initial rate v_0 and t_{50} value (the time required for the hydrolysis of 50% of the substrate) for the hydrolysis of oxacillin by synthesized zinc(II) complexes **1**–**3** were determined and compared with that of the known synthetic mimic for mβl, complex **4**. In a typical experiment, the incubation mixtures for the HPLC analysis contained oxacillin (1.06×10^{-3} M) and zinc(II) complexes(2.1×10^{-5} M) in 9:1 mixture of *N*-(2-hydroxyethyl) piperazine-*N*′-ethanesulfonic acid (HEPES) buffer/dimethyl sulfoxide (DMSO) at pH 7.5. The mixture was incubated at room temperature and aliquots (10 μl) injected onto the HPLC column and eluted with gradient solvent system (0.1% TFA in water–MeCN) using a C18 reverse-phase column. The oxacillin (retention time, 4.24 min) and the reaction product (oxacillin turnover product, retention time, 3.66 min) are separable. The decrease in the amount of oxacillin (μg) was calculated from the calibration plot. The chromatograms were extracted at 254 nm.

2.11. Phosphotriesterase assay

The hydrolysis of *p*-nitrophenyl diphenylphosphate (PNPDPP) by the zinc(II) complexes were determined by HPLC method [17]. The increase in the concentration of the hydrolyzed product, *p*-nitrophenol was followed by measuring the peak area of *p*-nitrophenol at 305 nm and the amount of *p*-nitrophenol present in the solution at a given time is determined from the calibration plot obtained by injecting known concentrations of *p*-nitrophenol. The initial rate v_0 and t_{50} value (the time required for the hydrolysis of 50% of the substrate) for the hydrolysis of *p*-nitrophenol by synthesized zinc(II) complexes **1**–**3** were determined and compared with that of the known synthetic mimic for PTE, complex **4**. In a typical experiment, the incubation mixtures for the HPLC analysis contained PNPDPP (10^{-3} M) and zinc(II) complexes(0.2×10^{-3} M) in 35% EtOH and 20×10^{-3} M *N*-cyclohexyl-2-aminoethanesulfonic acid (CHES) buffer at pH 9.0. The mixture was incubated at room temperature and aliquots (10 μl) injected onto the HPLC column and eluted with isocratic solvent system (80% Methanol and 0.1% TFA in water) using a C18 reverse-phase column. The *p*-nitrophenol, one of the reaction products (retention time, 3.78 min) and PNPDPP (retention time, 5.27 min) are separable. The increase in the amount of *p*-nitrophenol (μg) was calculated from the calibration plot. The chromatograms were extracted at 305 nm.

2.12. Comparison of metallo-β-lactamase and phosphotriesterase activities

In order to compare the mβl and PTE activities of the synthesized zinc(II) complexes, both the assays were carried out under identical conditions by using CHES buffer at pH 9.0 [17]. The mβl activities of complexes were determined by using 10^{-3} M oxacillin and 0.2×10^{-3} M zinc(II) complexes in 20×10^{-3} M CHES buffer at pH 9.0. The PTE activities of complexes were determined by using 10^{-3} M PNPDPP and 0.2×10^{-3} M zinc(II) complexes in 35% EtOH and 20×10^{-3} M CHES buffer at pH 9.0.

3. Results and discussion

3.1. Synthesis

The asymmetric phenolate-based ligands can be prepared either by sequential Mannich reaction of para-substituted phenol [25] or by the selective oxidation of one of the hydroxyl groups of 2,6-bis (hydroxymethyl)-4-methyl phenol [26]. We have synthesized the asymmetric ligands by the sequential Mannich reaction of para-substituted phenol, *p*-cresol with formaldehyde and two different amines. The reported procedure was slightly modified and ligands were prepared by following the method described in Scheme 2. As discussed earlier, the synthesis is complicated by the reversibility of Mannich reactions, and therefore, the formation of corresponding two symmetrical ligands was observed. The asymmetric ligand HL1, 2-((diethylamino)methyl)-6-((dimethylamino)methyl)-4-methyl phenol, was prepared as follows. In the first step, *N*,*N*-diethylamine, paraformaldehyde and *p*-cresol were refluxed in ethanolic solution. This led to the formation of both mono- and bi-aminoalkylated products, from which the mono-aminoalkylated product was separated by column chromatography. To the pure mono-aminoalkylated product, the second amine, *N*,*N*-dimethylamine and formaldehyde solution were added and the reaction was carried out under mild conditions and allowed to proceed for longer time. The second step was carried out under mild condition in order to minimize the reversibility of Mannich reaction that leads to the formation of the *p*-cresol under reaction conditions, which can possibly react with the amines present in the reaction medium to produce the corresponding symmetrical ligands. The ligand HL1 was separated from the corresponding symmetrical ligands by means of column chromatography. The asymmetric ligand HL2 was also prepared by using *N*,*N*-dipropylamine and *N*,*N*-dimethylamine. However, the symmetric ligands HL3 and HL4 were prepared by following the reported procedures [21]. The complexes **1**–**3** were prepared from ligands HL1–HL3,

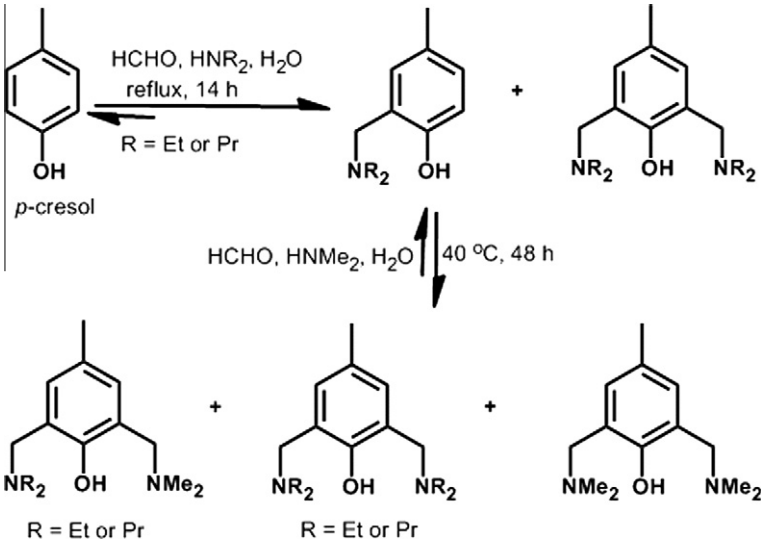

Scheme 2. Synthesis of symmetrical and unsymmetrical ligands by Mannich-type reactions.

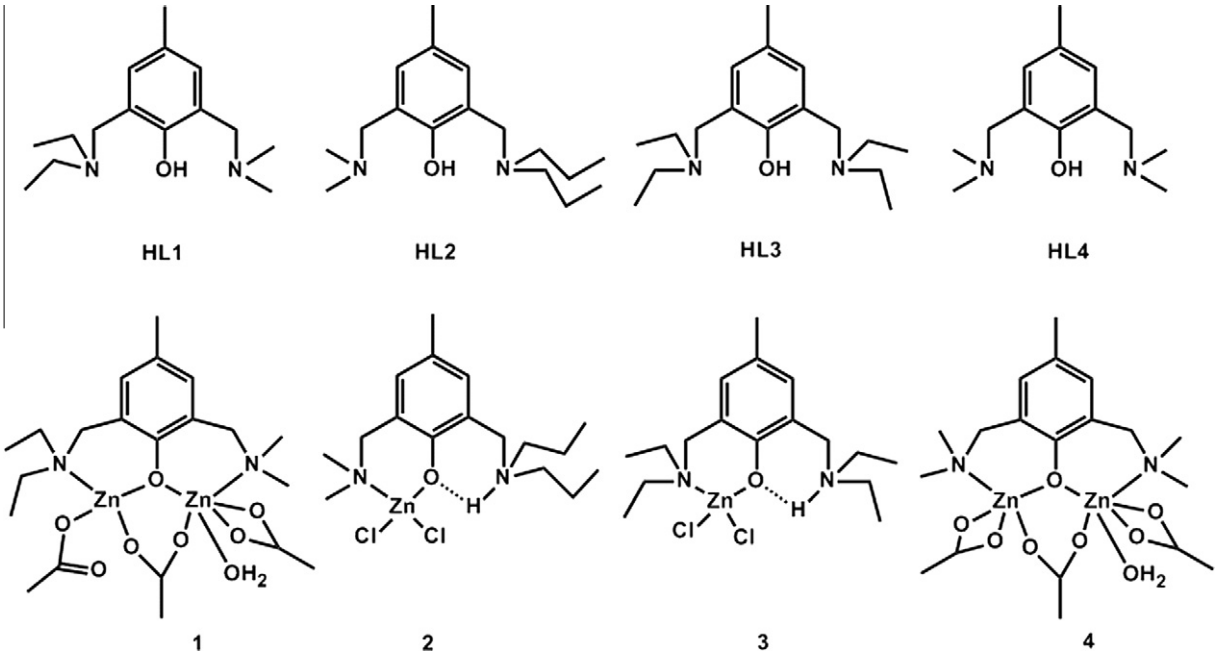

Fig. 2. Chemical structures of ligands HL1–HL4 and their corresponding zinc(II)complexes **1–4**.

respectively, by using reported procedure with slight modifications [15]. Complex **4**, which has been shown to be a synthetic mimic for mβl and PTE, was prepared for a comparison purpose [15]. The chemical structures of the ligands HL1–HL4 and complexes **1–4** are shown in Fig. 2.

3.2. X-ray crystal structure

The single crystals suitable for X-ray diffraction for complexes **1–3** are obtained from dichloromethane solution. The X-ray crystal structures of complexes **1–3** are shown in Fig. 3 and their crystallographic data are given in Table 1. The X-ray crystal structure of complex **1** reveals a binuclear zinc(II) complex. The two zinc(II) ions are in different co-ordination environments. The structure of this complex is similar to that of reported complex **4** obtained from a symmetrical ligand system. However, the co-ordination environment around Zn1 differs slightly in these two complexes, as the nature of coordination of the terminal acetate ligand is different. In complex **1**, the first zinc(II) ion (Zn1) is four co-ordinate with distorted tetrahedral geometry and is co-ordinated to three oxygen atoms and a nitrogen atom. The phenolate oxygen and an acetate ion act as bridging ligands, whereas the other asymmetric acetate (mono-dendate) and amino nitrogen act as terminal ligands. In both these complexes, the second zinc(II) ion (Zn2) is six co-ordinate with distorted octahedral geometry and is co-ordinated to five oxygen atoms and a nitrogen atom. In Zn2, the terminal acetate ion acts as a bidendate ligand and the sixth co-ordination is completed by a water molecule. The Zn···Zn distance in complex **1**, 3.398 Å is comparable to the Zn···Zn distances in complex **4** (3.355 Å) [15], mβl enzyme from species such as *Stenotrophomonas*

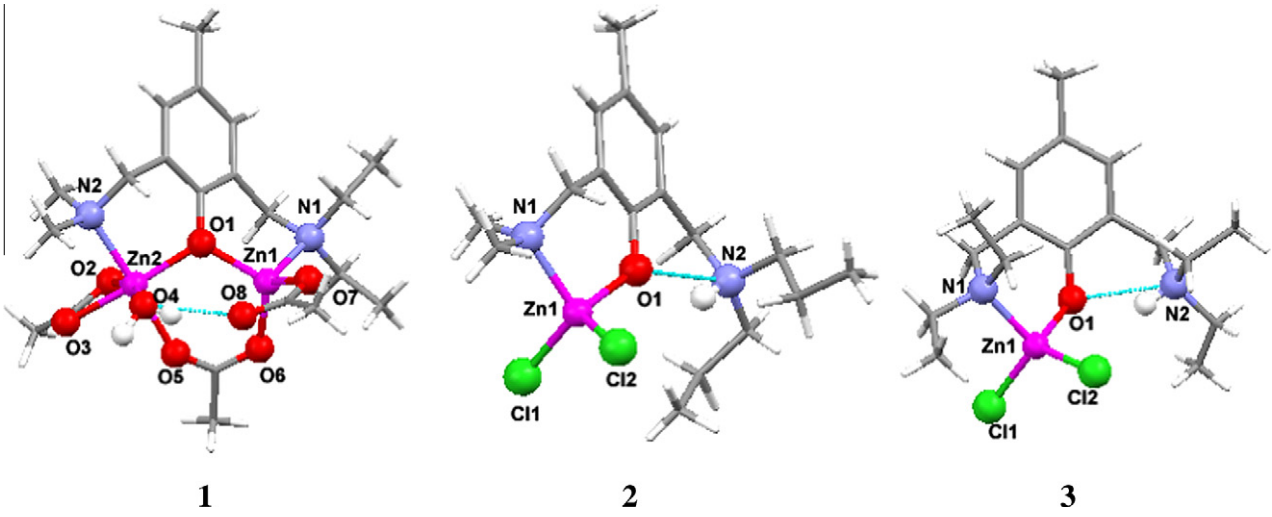

Fig. 3. X-ray crystal structures of complexes **1**–**3**. In **1**, the water molecule is hydrogen bonded to one of the acetate ligand, whereas in **3** and **4**, the amino nitrogen is hydrogen bonded to phenolate oxygen.

Table 1
Crystallographic data for complexes **1**–**3**.

Crystal data	Complex **1**	Complex **2**	Complex **3**
Empirical formula	$C_{21}H_{36}N_2O_8Zn_2$	$C_{17}H_{30}N_2OClZn$	$C_{17}H_{30}N_2OClZn$
Formula Weight	575.3	414.7	414.7
Crystal system	monoclinic	monoclinic	monoclinic
Space group	*C*2/*c*	*P*2(1)/*c*	*P*2(1)/*c*
a (Å)	26.3168(38)	9.1765(6)	17.9451(55)
b (Å)	14.2710(21)	20.2727(12)	8.0921(24)
c (Å)	17.6770(26)	11.0961(6)	14.4635(43)
α (°)	90.000(0)	90.000(0)	90.000(0)
β (°)	125.532(3)	97.590(2)	103.380(5)
γ (°)	90.000(0)	90.000(0)	90.000(0)
V (Å^3)	5402.68(143)	2046.15(6)	2043.29(27)
Z	8	4	4
D_{calc} (g cm^3)	1.41	1.35	1.35
Absorption coefficient (mm^{-1})	1.819	1.467	1.469
Reflections collected/ unique	23145/6361	16160/3828	16731/4818
F(0 0 0)	2399.5	871.8	871.8
R_{int}	0.099	0.042	0.089
R	0.055	0.064	0.090
R_w	0.094	0.099	0.235
Goodness-of-fit on F^2	0.944	1.163	1.076
$\Delta\rho_{min}$ and $\Delta\rho_{max}$ (e Å^{-3})	−0.344, 0.276	−0.341, 0.377	−0.735, 1.822

maltophilia (3.459 Å) [27], *Bacteroides fragilis* (3.457 Å) [28] and PTE (3.46 Å) [20]. However this Zn···Zn distance in complex **1** is shorter than that of binuclear mβl enzyme from *B. cereus* (3.848 and 4.365 Å) [29]. Complex **1** appears to be a good model for binuclear zinc(II) enzymes mβl and PTE as this complex posses a metal-bound water molecule similar to that in the active site of these enzymes. The metal-bound water molecule is hydrogen bonded to one of the acetate ion (O–H···O distance 2.624 Å). The crystal structures of complexes **2** and **3** obtained from asymmetric ligand HL2 and symmetric ligand HL3, respectively, inidicate the formation of mononuclear complexes. Although a different procedure was used, the structure of complex **3** was found to be identical to that reported by Habbadi et al. [21] The crystal structures of complexes **2** and **3** are similar to those obtained by Habbadi et al. for similar symmetrical ligand systems [21]. In these complexes, the zinc(II) ion is four co-ordinate with distorted tetrahedral co-ordination. Zinc(II) ion is co-ordinated to two chloride ions and phenolate oxygen and amino nitrogen from one of the arms of the ligand system. The phenolic proton is abstracted by the amino nitrogen atom of the non-coordinated arm of the ligand, which forms a positively charged ammonium group. The charge balance is provided by the negatively charged zinc(II) co-ordination sphere. The positively charged amino group is hydrogen bonded to the phenolate oxygen ion with N–H···O distances 2.636 Å and 2.696 Å in complexes **2** and **3,** respectively.

3.3. Metallo-β-lactamase activity of zinc(II) complexes

The mβl activities of the zinc(II) complexes were studied by following the hydrolysis of oxacillin, a β-lactam substrate. The mβl activities of the newly synthesized complexes **1–3** have been compared with that of complex **4**. The plots of % oxacillin vs time for the hydrolysis by zinc(II) complexes, free ligand, HL4 (one of the ligands) and zinc(II) acetate are given in Fig. 4 and the time required for the 50% hydrolysis of the substrate is given in Table 2. These data suggest that complex **1** is able to hydrolyze oxacillin completely with a t_{50} value of 158 min, which is very similar to that observed for complex **4** (126 min). This value is much lower than that of the control reaction or the reaction mediated by HL4 or zinc(II) acetate. The free ligand, HL4, does not show appreciable hydrolysis and only 24% hydrolysis was observed even after 1940 min. Although zinc(II) acetate showed a appreciable initial rate in

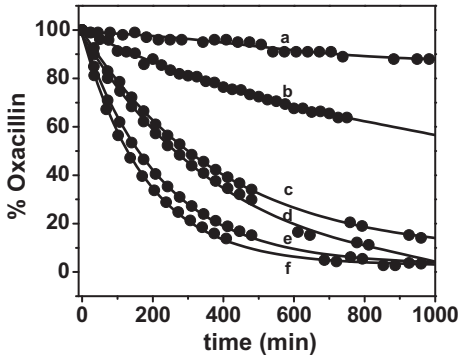

Fig. 4. Hydrolysis of oxacillin (1.06×10^{-3} M) by HL4 (a), zinc acetate (b), **2** (c), **3** (d), **1** (e) and **4** (f) (2.1×10^{-5} M) in DMSO:HEPES buffer (1:9), pH: 7.5. The reaction was followed by reverse-phase HPLC and the amount of oxacillin hydrolyzed at a given time was calculated from calibration plot.

Table 2
The t_{50} values and initial rates (v_0) for the hydrolysis of oxacillin by HL4, $Zn(OAc)_2{\cdot}2H_2O$ and complexes **1–4** at room temperature.

Catalyst	Oxacillin	
	t_{50} (min)[a]	v_0 (μM min^{-1})[e]
Control	>6300[b]	0.76
HL4	>1940[c]	0.32
$Zn(OAc)_2{\cdot}2H_2O$	>750[d]	0.81
1	158.1	4.12
2	299.0	2.35
3	262.1	2.79
4	125.6	4.79

[a] The time required for the 50% hydrolysis of the substrate t_{50} was determined by monitoring the decrease in the peak area of oxacillin. [oxacillin]: 1.06×10^{-3} M; [catalyst]: 2.12 x 10^{-5} M in DMSO/HEPES buffer (1:9), pH 7.5.
[b] After 6300 min, only 36% hydrolysis was observed.
[c] After 1940 min, only 24% hydrolysis was observed.
[d] After 750 min, only 36% hydrolysis was observed.
[e] The initial rate v_0 was calculated from initial 5–10% of the reaction, by monitoring the decrease in peak area of oxacillin.

comparison with metal-free systems, it is capable of hydrolyzing only 36% even after 750 min. This can be attributed to the inhibition of free zinc(II) ions in solution by the products. However, no such inhibition was observed in the case of dinuclear zinc(II) complex **1** as the metal ions are tightly bound in the well-organized ligand system.

The efficient hydrolysis of oxacillin by complex **1** can be attributed to the two tightly bound zinc(II) ions. As in the case of **4**, complex **1** also possesses the metal-bound water molecule, which is essential for the catalytic activity. The Zn2-bound water molecule is activated through a hydrogen bonding (O-H···O, 2.624 Å) with the oxygen atom of the acetate ion coordinated to Zn1. This is in accordance with the activation of metal-bound water molecule in the active site of the mβl enzyme by amino acid residue such as Asp-120, which acts as a general base. The minor variation in the structure of ligands in complexes **1** and **4** does not appear to change the catalytic activity significantly. Therefore, the metal-bound water molecule in both these complexes is responsible for their catalytic efficiency. The zinc(II) complexes **2** and **3,** which lacks metal-bound water molecule, exhibited almost two-times higher t_{50} values as compared to complexes **1** and **4** having metal-bound water molecule. However, the ability of mononuclear zinc(II) complexes **2** and **3** to hydrolyze oxacillin suggests that the presence of second zinc(II) ion is not important for the initial hydrolysis of β-lactam. This is in accordance with the observation of Kaminskaia et al. that the presence of second zinc ion is not crucial for the β-lactamase activity [30].

3.4. Phosphotriesterase activity of zinc(II) complexes

As mβl and PTE possess similar active sites with metal-bound water molecule, we have studied the synthesized zinc(II) complexes for their ability to hydrolyze organophosphotriester, PNPDPP. The initial rate (v_0) and t_{50} values for the hydrolysis of PNPDPP by zinc(II) complexes to produce *p*-nitrophenol are given in Table 3, and the plots of % *p*-nitrophenol vs time are shown in Fig. 5. Interestingly, complexes **3** and **4** having zinc-bound chloride ions exhibited much better activity than complexes **1** and **2** having zinc-bound water molecule. This can be attributed to the replacement of labile chloride ions in **3** and **4** by hydroxide ion in CHES buffer at pH 9.0. This is in accordance with our previous observations that the metal-bound chloride ions are replaced by hydroxide ions in CHES buffer [17]. These metal-bound hydroxide ions act as nucleophile in the hydrolytic reactions. The binuclear complex **1** exhibited lower PTE activity as that of reported complex **4**, which

Table 3
The t_{50} values and initial rates (v_0) for the hydrolysis of PNPDPP by zinc(II) complexes **1–4** at room temperature.

Catalyst	PNPDPP	
	t_{50} (min)[a]	v_0 (μM min^{-1})[c]
Control	>7094[b]	0.020
1	6180.3	0.1389
2	4731.4	0.1611
3	5174.9	0.1490
4	5912.2	0.1535

[a] The time required for the 50% hydrolysis of the substrate t_{50} was determined by monitoring the increase in the peak area of *p*-nitrophenol. [PNPDPP]: 0.2×10^{-3} M; [catalyst]: 0.2×10^{-3} M in 35% ethanol and CHES buffer, pH 9.0.
[b] After 7094 min, only 30% hydrolysis was observed.
[c] The initial rate v_0 was calculated from initial 5–10% of the reaction, by monitoring the increase in the peak area of *p*-nitrophenol.

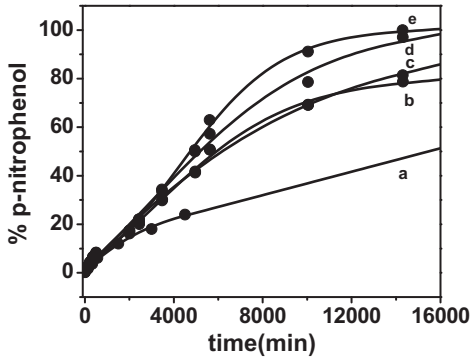

Fig. 5. Hydrolysis of PNPDPP (0.20×10^{-3} M) by control (a), **4** (b), **1** (c), **3** (d) and **2** (e) (2.1×10^{-5} M) in 35% ethanol and 20 mM CHES buffer, pH 9.0. The reaction was followed by reverse-phase HPLC and the amount of *p*-nitrophenol formed at a given time was calculated from the calibration plot.

can be ascribed to the inhibition of the complex by the hydrolyzed product, diphenyl phosphate (DPP) [17]. The replacement of bridging acetate by DPP has been previously observed in complex **4** [17]. As in the case of mβl activity, the slight change in ligand system on moving from **1** to **4** or **2** to **3** does not show significant change in PTE activity.

Table 4
Comparison of mβl and PTE activity of the synthesized zinc(II) complexes.

Catalyst	mβl activity		PTE activity	
	t_{50} (min)[a]	v_0 (μM min^{-1})[c]	t_{50} (min)[d]	v_0 (μM min^{-1})[f]
Control	>1885[b]	0.09	>2800[e]	0.020
1	156.8	13.54	6180.3	0.1389
2	170.3	12.60	4731.4	0.1611
3	317.5	8.44	5174.9	0.1490
4	103.8	18.23	5912.2	0.1535

[a] The time required for the 50% hydrolysis of the substrate t_{50} was determined by monitoring the decrease in the peak area of oxacillin. [oxacillin]: 1.0×10^{-3} M; [catalyst]: 0.2×10^{-3} M in CHES buffer, pH 9.0.
[b] After 1885 min, only 29% of hydrolysis of oxacillin was observed.
[c] The initial rate v_0 is calculated from the initial 5–10% of the reaction by following the decrease in peak area of oxacillin.
[d] The time required for the 50% hydrolysis of the substrate t_{50} was determined by monitoring the increase in the peak area of *p*-nitrophenol. [PNPDPP]: 1.0×10^{-3} M; [catalyst]: 0.2×10^{-3} M in 35% ethanol and CHES buffer, pH 9.0.
[e] After 2880 min, only 71% of hydrolysis of PNPDPP was observed.
[f] The initial rate v_0 is calculated from the initial 5–10% of the reaction by following the increase in peak area of *p*-nitrophenol.

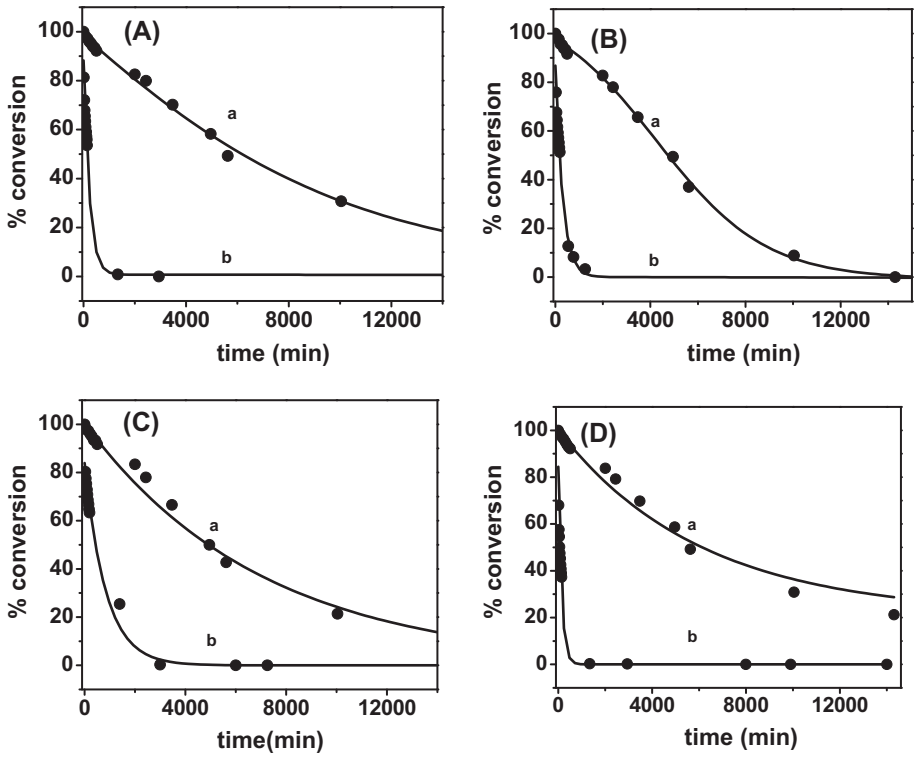

Fig. 6. Comparison of PTE and mβl activities of (A) complex **1** (B) complex **2** (C) complex **3** and (D) complex **4**. Plots a and b represent PTE and mβl activities, respectively. Hydrolysis of oxacillin and PNPDPP were carried out in 20 mM CHES buffer, pH 9.0. For PTE assay 35% ethanol was used to dissolve PNPDPP. [oxacillin] or [PNPDPP]: 1×10^{-3} M and [catalyst]: 0.2×10^{-3} M.

3.5. Comparison between mβl and PTE activities of zinc(II) complexes

To compare the mβl and PTE activities of complexes **1**–**4**, both the mβl and PTE assays were carried out under identical conditions in CHES buffer at pH 9.0. The substrate:catalyst concentration was kept at 5:1. The initial rates (v_0) and t_{50} values for the hydrolysis of PNPDPP or oxacillin by zinc(II) complexes are given in Table 4, and the plots of % conversion vs time is shown in Fig. 6. In the presence of complexes **1**–**4**, the hydrolysis of oxacillin was found to be much higher than that of PNPDPP, indicating that complexes **1**–**4** are better mβl mimics than PTE mimics. Among these four complexes, the mβl activity of **1** and **4** was found to be higher than that of complexes **2** and **3**. This can be ascribed to the two tightly bound zinc(II) ions and also to the presence of activated water molecules. However, the increase in PTE activity of **2** and **3** can be attributed to the replacement of labile chloride ion by hydroxide ion under assay condition. As discussed earlier, the decrease in PTE activity of **1** and **4** is possibly due to an inhibition by DPP [17].

4. Conclusions

In this paper, we have described the synthesis of a few asymmetric phenolate-based ligands and their corresponding zinc(II) complexes. These complexes were studied for their mβl and PTE activities. In agreement with our previous studies on mβl mimics, a binuclear zinc(II) complex having a water molecule exhibits high mβl activity. Although the mononuclear zinc(II) complexes **2** and **3** exhibit considerable mβl activity, the activity is almost two times lower than that of the binuclear zinc(II) complexes. As the active sites of both mβl and PTE possess zinc(II)-bound water molecule, these complexes were also studied for their PTE activity. All the four complexes exhibited higher mβl activity than PTE activity. In contrast to the mβl activity, the mononuclear complexes exhibited much higher PTE activity, indicating that the replacement of the metal-bound labile chloride ions by hydroxide ions is important for the PTE activity. The poor PTE activity of the binuclear zinc(II) complexes can be ascribed to the inhibition by the hydrolyzed product, diphenyl phosphate.

Acknowledgements

This study was supported by the Department of Science and Technology (DST), New Delhi. GM acknowledges the DST for the award of Ramanna and Swarnajayanti fellowships. MU thanks the Indian Institute of Science (IISc) for a research fellowship.

Appendix A. Supplementary material

The supplementary data include ^{1}H NMR, ^{13}C NMR and mass spectra of the ligands. CCDC 797091, 797090 and 797092 contain the supplementary crystallographic data for complexes **1**, **2** and **3**, respectively. These data can be obtained free of charge from The Cambridge Crystallographic Data Centre via www.ccdc.cam.ac.uk/data_request/cif. Supplementary data associated with this article can be found, in the online version, at doi:10.1016/j.ica.2011.03.064.

References

[1] R.J.P. Williams, in: C.F. Mills (Ed.), Zinc in Human Biology, Springer-Verlag, Berlin, Germany, 1989, p. 15.
[2] B.L. Vallee, in: I. Bertini, H.B. Gary (Eds.), A Synopsis of Zinc Biology and Pathology in Zinc Enzymes, Birkhauser, Boston, 1986.
[3] H. Vahrenkamp, Dalton Trans. 42 (2007) 4751.
[4] (a) N. Sträter, W.N. Lipscomb, T. Klabunde, B. Krebs, Angew. Chem. 108 (1996) 2158;
(b) N. Sträter, W.N. Lipscomb, T. Klabunde, B. Krebs, Angew. Chem., Int. Ed. Engl. 35 (1996) 2025;
(c) H. Steinhagen, G. Helmchem, Angew. Chem. 108 (1996) 2489;

(d) H. Steinhagen, G. Helmchem, Angew. Chem., Int. Ed. Engl. 35 (1996) 2339;
(e) D.E. Wilcox, Chem. Rev. 96 (1996) 2435;
(f) W.N. Lipscomb, N. Sträter, Chem. Rev. 96 (1996) 2375.
[5] J. Weston, Chem. Rev. 105 (2005) 2151.
[6] M.W. Crowder, J. Spencer, A.J. Vila, Acc. Chem. Res. 39 (2006) 721 (and references therein).
[7] M.I. Page, A. Badarau, Bioinorg. Chem. Appl. 2008 (2008) 1 (and references therein).
[8] J. Dragun, A.C. Kuffner, R.W. Schneiter, Chem. Eng. 91 (1984) 65.
[9] D.B. Barr, R. Bravo, G. Weerasekera, L.M. Caltabiano, R.D. Whitehead, A.O. Olsson, S.P. Caudill, S.E. Schober, J.L. Pirkle, E.J. Sampson, R.J. Jackson, L.L. Needham, Environ. Health Perspect. 112 (2004) 186.
[10] J.E. Casida, G.B. Quistad, Chem. Res. Toxicol. 17 (2004) 983.
[11] M. Lotti, Toxicology 181 (2002) 245.
[12] B.K. Singh, Nat. Rev. Microbiol. 7 (2009) 756.
[13] (a) N. Sethunathan, T.J. Yoshida, Microbiology 19 (1973) 873;
(b) C.M. Serdar, D.T. Gibson, D.M. Munnecke, J.H. Lancaster, Appl. Environ. Microbiol. 44 (1982) 246;
(c) G. Amitai, R. Adani, G. Sod-Moriah, I. Rabinovitz, A. Vincze, H. Leader, B. Chefetz, L. Leibovitz-Persky, D. Friesem, Y. Hadar, FEBS Lett. 438 (1998) 195;
(d) H. Shim, F.M. Raushel, Biochemistry 39 (2000) 7357.
[14] Y.-J. Dong, M. Bartlam, L. Sun, Y.-F. Zhou, Z.-P. Zhang, C.-G. Zhang, Z. Rao, X.-E. Zhang, J. Mol. Biol. 353 (2005) 655.
[15] A. Tamilselvi, G. Mugesh, Chem. Eur. J. 12 (2006) 7797.
[16] A. Tamilselvi, G. Mugesh, J. Biol. Inorg. Chem. 13 (2008) 1039.
[17] A. Tamilselvi, G. Mugesh, Chem. Eur. J. 16 (2010) 8878.
[18] A. Carfi, S. Pares, E. Duee, M. Galleni, C. Duez, J.M. Frère, O. Dideberg, EMBO J. 14 (1995) 4914.
[19] S.M. Fabiane, M.K. Sohi, T. Wan, D.J. Payne, J.H. Bateson, T. Mitchell, B. Sutton, Biochemistry 37 (1998) 12404.
[20] M.M. Benning, H. Shim, F.M. Raushel, H.M. Holden, Biochemistry 40 (2001) 2712.
[21] N. Habbadi, M. Dartiguenave, L. Lamande, M. Sanchez, M. Simard, A.L. Beauchampd, A. Souiria, New J. Chem. (1998) 983.
[22] SMART, Version 5.05, Bruker AXS, Madison, 1998.
[23] (a) G.M. Sheldrick, SHELXTL V97-2, Siemens Industrial Automation Inc., Madison, 1997.;
(b) G.M. Sheldrick, SHELX-97, Program for Crystal Structure Solution and Refinement, University of Göttingen, Göttingen, Germany, 1997.
[24] G.M. Sheldrick, SADABS, Version 2, Multi-Scan Absorption Correction Program, University of Göttingen, Göttingen, Germany, 2001.
[25] (a) M. Lubben, B.L. Feringa, J. Org. Chem. 59 (1994) 2227;
(b) T.M. Rajendiran, R. Kannappan, R. Mahalakshmy, J. Rajeswari, R. Venkatesan, P. Rao, Transition Met. Chem. 28 (2003) 447;
(c) R. Mahalakshmy, R. Venkatesan, P.S. Rao, R. Kannappan, T.M. Rajendiran, Transition Met. Chem. 29 (2004) 623.
[26] (a) E. Lambert, B. Chabut, S.C. Noblat, A. Deronzier, G. Chottard, A. Bousseksou, J.-P. Tuchagues, J. Laugier, M. Bardet, J.-M. Latour, J. Am. Chem. Soc. 119 (1997) 9424;
(b) M. Jarenmark, S. Kappen, M. Haukka, E. Nordlander, Dalton Trans. (2008) 993.
[27] (a) J.A. Cricco, E.G. Orellano, R.M. Rasia, E.A. Ceccarelli, A.J. Vila, Coord. Chem. Rev. (1999) 190;
(b) J.A. Cricco, E.G. Orellano, R.M. Rasia, E.A. Ceccarelli, A.J. Vila, Coord. Chem. Rev. (1999) 519.
[28] N.O. Concha, B.A. Rasmussen, K. Bush, O. Herzberg, Structure 4 (1996) 823.
[29] J.A. Cricco, A.J. Vila, Curr. Pharm. Des. 5 (1999) 915.
[30] N.V. Kaminskaia, B. Spingler, S.J. Lippard, J. Am. Chem. Soc. 122 (2000) 6411.